CHAPTER 5

PERFORMANCE ENHANCEMENT USING CLUSTERED-CAVITY GYROKLYSTRON — A PRELIMINARY STUDY

PERFORMANCE ENHANCEMENT USING CLUSTERED-CAVITY GYROKLYSTRON — A PRELIMINARY STUDY

5.1. Introduction

Recent development in the radar applications has focused on narrow-band gyroklystrons (bandwidth < 1GHz) which is operating in Ka-band, and W-band and generates RF peak power of up to 100kW. But, the advanced high-resolution imaging radar applications require more versatile tubes operating at stable, high power and with large bandwidth up to 1-5GHz, because if the gyroklystron is to be used as a radar, bandwidth is directly related to radar resolution as $\Delta R = c / 2\Delta f$, where ΔR is the range resolution, and Δf is the bandwidth. The instantaneous bandwidth of the gyroklystron amplifier is determined by the quality factor (Q) of the cavities and mainly by the output cavity. This leads to the narrow bandwidth of the existing gyroklystron amplifiers, i. e., limited to 0.1-1.4% which is mainly because of the limited quality factor (150 to 300) of the cavity.

Nowadays, various techniques have been employed for the enhancement of bandwidth of the gyroklystron device. Firstly, the method of stagger tuning is employed in conventional klystrons [Stapran *et al.* (1973)] in which the bandwidth can be significantly increased by detuning the resonant Eigen frequencies of cavities. Then, the theory of stagger tuned devices is widely applied to gyroklystron amplifiers to broaden their bandwidth but at the cost of reduction of gain of the device [Nusinovich *et al.* (1997)]. Therefore, the tradeoff in the gain and bandwidth should be analyzed. Even though, with stagger-tuning, the bandwidth of gyroklystron can be broadened to only some extent.

Later on, a new gyro-device interaction circuit, containing the clustered cavities is employed to figure out the complication of narrow bandwidth associated with cavity-related gyro-amplifiers with minimum degradation of gain and efficiency. The clustered-cavity approach for gyro-amplifiers was initially proposed by H. Guo *et al.* in 2000 at the HPM teleconference [Guo *et al.* (2000)]. The technique is highly utilized for improving both the efficiency and bandwidth of these devices. The clustered-cavity approach was first applied to the conventional klystrons by Symons and Vaughan in 1994 for improving its bandwidth [Symons and Vaughan (1994)]. The only difference is that the clustered-cavity gyroklystron operates in the transverse electric (TE) mode while its counterpart viz. Symons' clustered-cavity klystron operates in the transverse magnetic (TM) mode. Further, azimuthal bunching occurs in the clustered-cavity gyroklystron whereas the clustered-cavity klystron experiences the electron bunching in the axial direction. The clustered-cavity approach would improve the bandwidth of all cavity related gyro-amplifiers such as gyroklystrons, gyrotwystrons, and inverted gyrotwystrons (phigtrons) and hence results in the significant enhancement in the performance of narrowband millimeter-wave gyro-amplifiers.

The fundamental concept of this configuration is that the individual intermediate cavities of a gyroklystron is replaced by doublets or triplets of artificially loaded cavities having Q-factors of each cavity in a cluster is reduced to one-half or one-third of the single cavity they replace. The overall dimension of the tube remains unchanged. Thus, for a clustered-cavity device, the bandwidth is either doubled or tripled that of the single cavity device. For example, for the case of two-cavity the bandwidth can be doubled. Figure 5.1 shows the schematic of a two-clustered gyroklystron. In practice, there are some important issues which should be addressed while using clustered cavities to a gyro-amplifier.

Mainly, the individual sub-cavities in each cluster should be as close as possible so that the significant coupling between the adjacent cavities is diminished. To achieve this, i. e., minimum coupling between the cavities in each cluster, firstly the diameter of the cavity end is cut off for the operating mode. Additionally, for indulging more appropriate isolation, highly lossy ceramic materials are used as absorbers to eliminate possible coupling between sub-units.

The effect of cluster-cavities on the performance of the gyroklystron has been reported in the literature by many authors. In the year 2002, the applicability of cluster-cavity in the fundamental harmonic gyro-amplifiers was analytically studied [Nusinovich *et al*. (2002)]. A 35GHz, two-cavity NRL gyroklystron amplifier [Choi *et al.* (1998)] has been analyzed to highlight the benefits of cluster-cavity concept. The enhancement of bandwidth from 0.34% to about 1.2% is observed which clearly indicates the performance improvement of the device. The one-to one comparison of the conventional cavity and clustered-cavity gyroklystron, i. e., total number of cavities remains equal was presented in 2003. A conventional four-cavity and three-stage clustered-cavity gyroklystron is considered for the analysis. The result shows that the former tube has a slightly higher efficiency, while the later has advantages in its bandwidth properties, gain, and the gain-bandwidth product [Sinitsyn *et al.* (2003)]. Later on, an analytical concept has been developed to maximize the harmonic current and optimize the drift section length in the frequency multiplying clustered-cavity gyro-amplifiers. In addition, simulation has been performed to benchmark with the theory and to further investigate the detailed performance characteristics of the cluster-cavity gyro-amplifiers [Miao *et al.* (2004)].

This chapter of the thesis is organized as follows. In Section 5.2, the analysis of the clustered-cavity gyroklystron amplifier is presented. The design parameters considered for

the analysis are discussed in Section 5.3. Computational results obtained are described in Subsection 5.3.1a and are compared with the earlier reported experimental values [Zasykin *et al.* (2006)]. Further, device PIC simulation is performed using CST particle studio to validate the analytical values obtained and the results are discussed in Subsection 5.3.1b. The relevant conclusions are drawn in Section 5.4.

5.2. Clustered-Cavity Analysis

5.2.1. General Formalism

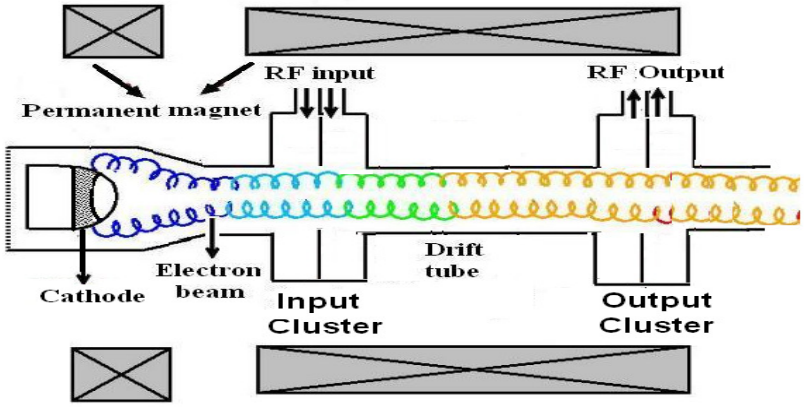

Figure. 5.1: Schematic of a two-clustered gyroklystron amplifier.

Let the amplitude and phase of field in a cavity can be expressed as $F_{k,l} = \left|F_{k,l}\right| e^{i\psi_{k,l}}$, where k indicates the cluster number, and l indicates the number of cavities in a given cluster, which can be evaluated from the balance equations.

The balance equation for the input cluster can be given as:

$$F_{k,l}\left\{1 + i\delta_{k,l} + iI_{0(k,l)}\chi_{k,l}\right\} + A_l = 0 \quad . \tag{5.1}$$

Let $A^2 = \sum_l A_l^2$ is the overall field intensity in the input cluster excited by the input driver and it is expressed in terms of driver power P_{in} as [Nusinovich *et al.* (1997)]:

$$\left|A\right|^2 = \frac{4I_{01}P_{in}Q_1}{P_{0\perp}Q_{cpl}} \quad , \tag{5.2}$$

where, Q_{cpl} is the external quality factor or coupling of the input cavity, Q_1 is the loaded quality factor, $P_{0\perp} = [\beta_{\perp 0}^2 / 2(1-\gamma_0^{-1})] V_b I_b$ is the electron beam power. A_l is the complex field amplitude excited in the l^{th} cavity of the input cluster by driver, so $A_l \neq 0$ for the first cluster and can be expressed as $A_l = |A_l| e^{i\phi_s}$.

For other cavities in the cluster, $A_l = 0$, so from equation (5.1) the balance equations can be written as:

$$I_{0(k,l)} \chi''_{k,l} = 1, \;\; I_{0(k,l)} \chi'_{k,l} = -\delta_{k,l} \;\; . \tag{5.3}$$

Here $\chi_{k,l}$ is the electron beam susceptibility with reference to the cavity field and is expressed as:

$$\chi_{k,l} = -i - \frac{2i}{F_{k,l}} \sum_{l'<l} F_{k,l'} - \frac{2i}{F_{k,l}} \left\langle e^{-i\theta_{dr,k-1}} \right\rangle \quad , \tag{5.4}$$

where, the foremost term indicates the effect of beam loading. The secondary term indicates the effect of previous cavities in a particular cluster (In case of conventional gyroklystron, this term is zero, since l = 0). The third term indicates the consequence of ballistic bunching of electrons which is zero for the case of input cluster, due to the uniform phase distribution of electrons at the entrance.

1. Field in the Input Cluster $\left(F_{1,\Sigma}\right)$

The total field in the input cluster is expressed as:

$$F_{1,\Sigma} = |F_{1,1}| e^{i\psi_{1,1}} + |F_{1,2}| e^{i\psi_{1,2}} \quad . \tag{5.5}$$

The electron beam susceptibility with reference to the resonator field in the first cavity of the input cluster can be expressed as:

$$\chi_{1,1} = -i \quad . \tag{5.6}$$

The complex field in the first cavity of the input cluster can be determined from the balance equation (5.1) and can be expressed as [Nusinovich *et al.* (2002)]:

$$\left|F_{1,1}\right|e^{i\psi_{1,1}} = \frac{\left|A_1\right|e^{i\phi_s}}{\left(1+I_{0(1,1)}\right)+i\,\delta_{1,1}} \quad , \tag{5.7}$$

where, $I_{0(1,1)}$ is the normalized beam current parameter given by [Nusinovich *et al.* (2002)]:

$$I_{0(1,1)} = \frac{e\,I_b\,Q_{1,1}}{m_e\,c^3\,\gamma_0}\left(\frac{2^2}{(2-1)!}\right)^2 \beta_{\perp 0}^{-2} \times \frac{J_{m\mp 2}^2\left\{k_{nt}R_b\right\}}{(x_{mn}'^2-m^2)J_m^2\{v\}\int\left|f\right|^2 dz'} \quad , \tag{5.8}$$

where, function $f\{\xi\}$ gives the axial cavity field profile, I_b is the beam current, x'_{mn} is the eigenvalue of a TE_{mn} mode of a cylindrical cavity, $\delta_{1,1}$ is the detuning between the signal frequency ω_s and the eigenfrequency of the cavity $\omega_{1,1}$ and is given by:

$$\delta_{1,1} = \frac{\left(\omega_s-\omega_{1,1}\right)\times 2Q_{1,1}}{\left(\omega_{1,1}\right)} \quad . \tag{5.9}$$

Similarly, the susceptibility with reference to field in the second cavity of the input cluster is expressed as:

$$\chi_{1,2} = -i-2i\frac{\left|F_{1,1}\right|}{\left|F_{1,2}\right|}e^{i\left(\psi_{1,1}-\psi_{1,2}\right)} \quad , \tag{5.10}$$

which being combined with equation (5.1) gives the field in the second cavity of the input cluster [Nusinovich *et al.* (2002)]:

$$\left|F_{1,2}\right|e^{i\psi_{1,2}} = \frac{\left|A_1\right|+2I_{0(1,2)}\left|F_{1,1}\right|e^{i\left(\psi_{1,1}-\phi_s\right)}}{\left(1+I_{0(1,2)}\right)+i\,\delta_{1,2}} \quad . \tag{5.11}$$

When all the cavities of the input cluster oscillate in phase,

$$\left|F_{1,\Sigma}\right| = \sum_{l \le L_1} \left|F_{1,l}\right| = \left|F_{1,1}\right| + \left|F_{1,2}\right| \quad , \tag{5.12}$$

where, L_1 is the number of cavities in the input cluster. For small beam loading, $I_{0(1,1)} = I_{0(1,2)} = I_{01}$ and zero detuning ($\delta_{1,1} = \delta_{1,2} = 0$), the total field amplitude in the input cluster is expressed as:

$$\left|F_{1,\Sigma}\right| = 2\left|A_1\right|\left(1+2I_{01}\right)/\left(1+I_{01}\right)^2 \quad . \tag{5.13}$$

2. Drift Section Length

The optimum drift section length is given as:

$$\mu_{dr,opt}^{(2)} \simeq 0.4\mu_{dr} \quad , \tag{5.14}$$

where, μ_{dr} is the normalized drift section length of the conventional gyroklystron amplifier and superscript (2) indicates the number of cavities in the input cluster. Now, the bunching parameter (q) which is used to determine the electron phase angles at the input of the second cluster can be calculated as:

$$q = 2\left|F_{1,\Sigma}\right|\mu_{dr,opt}^{(2)} \quad . \tag{5.15}$$

3. Field in the Output Cluster $\left(F_{2,\Sigma}\right)$

The total field in the output cluster is expressed as:

$$F_{2,\Sigma} = \left|F_{2,1}\right|e^{\psi_{2,1}} + \left|F_{2,2}\right|e^{\psi_{2,2}} \quad . \tag{5.16}$$

The electron beam susceptibility with reference to the resonator field in the first cavity of the output cluster can be expressed as:

$$\chi_{2,1} = -i - 2i\frac{J_1\{q\}e^{-i(\psi_{2,1}-\phi_s)}}{\left|F_{2,1}\right|} \quad . \tag{5.17}$$

Equation (5.10) being combined with balance equation (5.3), gives the complex field in the first cavity of the output cluster [Nusinovich *et al.* (2002)]:

$$\left|F_{2,1}\right| e^{i\left(\psi_{2,1}-\phi_s\right)} = \frac{-2I_{0(2,1)}J_1\{q\}}{\left(1+I_{0(2,1)}\right)+i\,\delta_{2,1}} \quad . \tag{5.18}$$

Similarly, the susceptibility with reference to field in the second cavity of the output cluster is given by:

$$\chi_{2,2} = -i - 2i\frac{\left|F_{2,1}\right|}{\left|F_{2,2}\right|} e^{i\left(\psi_{2,1}-\psi_{2,2}\right)} - 2i\frac{J_1\{q\}e^{-i\left(\psi_{2,2}-\phi_s\right)}}{\left|F_{2,2}\right|} \quad , \tag{5.19}$$

which gives the complex field in the second cavity of the output cluster:

$$\left|F_{2,2}\right| e^{i\left(\psi_{2,2}-\phi_s\right)} = -2J_1\{q\}I_{0(2,2)}\left(\frac{1-I_{0(2,1)}+i\,\delta_{2,1}}{\left(1+I_{0(2,1)}+i\,\delta_{2,1}\right)\left(1+I_{0(2,2)}+i\,\delta_{2,2}\right)}\right) \quad . \tag{5.20}$$

When all the cavities of the output cluster oscillate in phase,

$$\left|F_{2,\Sigma}\right| = \sum_{l \le L_2} \left|F_{2,l}\right| = \left|F_{2,1}\right| + \left|F_{2,2}\right| \quad , \tag{5.21}$$

where, L_2 is the number of cavities in the output cluster. For the case of small beam loading, $I_{0(2,1)} = I_{0(2,2)} = I_{02}$ and small pre-bunching in input cavity ($J_1(q) \approx q/2$), the total field amplitude in the output cluster is expressed as:

$$\left|F_{2,\Sigma}\right|^2 = \left(2qI_{02}\right)^2 \frac{1+\left[\left(\delta_{2,1}+\delta_{2,2}\right)/2\right]^2}{\left(1+\delta_{2,1}^2\right)\left(1+\delta_{2,2}^2\right)} \quad . \tag{5.22}$$

4. Transverse Efficiency ($\eta_\perp$) and Gain (G)

In the case of absence of stagger tuning between the cavities of the output cluster, $\eta_\perp$ of the two-clustered gyroklystron is computed by the expression:

$$\eta_\perp = -2J_1\left\{q_\Sigma\right\}\left(\left|F_{2,\Sigma}\right|\right) - \left|F_{2,\Sigma}\right|^2 \quad . \tag{5.23}$$

The gain (G) of the device is given by:

$$G = 10\log\left\{\frac{1}{A^2}\sum_{l=1}^{L_k}\left|F_{k,l}^{2}\right|\right\} \quad . \tag{5.24}$$

5.2.2. Stagger-Tuned Clustered-Cavity Gyroklystron

The variable part of gain $G_{ss}^{(\mathrm{var})}$ versus normalized frequency detuning δ has been plotted to analyze the stagger tuning effect on the bandwidth and gain of clustered-cavity gyroklystron. The bandwidth of the device is represented in terms of δ. The gain of the device is expressed as:

$$G = G_{ss}^{(const)} + G_{ss,1}^{(\mathrm{var})} + G_{ss,2}^{(\mathrm{var})} = G_{ss}^{(const)} + G_{ss}^{(\mathrm{var})} \quad , \tag{5.25}$$

where, $G_{ss,1}^{(\mathrm{var})}$ and $G_{ss,2}^{(\mathrm{var})}$ are the signal frequency tuning and stagger-tuning effects in the input and output cluster and are given by [Nusinovich *et al.* (2002)]:

$$G_{ss,1}^{(\mathrm{var})} = 10\log\left\{\frac{1}{2(1+\hat{\delta}_{1,1}^{2})} + \frac{1}{2\left(1+\hat{\delta}_{1,2}^{2}\right)} + \frac{I_1\left(2+I_1\right)}{2\left(1+\hat{\delta}_{1,1}^{2}\right)\left(1+\hat{\delta}_{1,2}^{2}\right)} + \right. \quad , \tag{5.25}$$
$$\left. \frac{1}{\sqrt{\left(1+\hat{\delta}_{1,1}^{2}\right)\left(1+\hat{\delta}_{1,2}^{2}\right)}} \times \sqrt{\left(1+\frac{I_1\left(2+I_1\right)}{1+\hat{\delta}_{1,1}^{2}}\right)}\cos\left(\psi_{1,2}-\psi_{1,1}\right)\right\}$$

$$G_{ss,2}^{(\mathrm{var})} = 10\log\left\{\frac{1}{1+\hat{\delta}_{2,1}^{2}} + \frac{1}{1+\hat{\delta}_{2,2}^{2}}\left[1+\frac{I_2\left(2+I_2\right)}{1+\hat{\delta}_{2,1}^{2}}\right]\right\} \quad , \tag{5.26}$$

$$\cos\left(\psi_{1,2}-\psi_{1,1}\right) = \frac{A - 2I_1\hat{\delta}_{1,1}\hat{\delta}_{1,2} + \hat{\delta}_{1,1}\left(2I_1\hat{\delta}_{1,1} + A\hat{\delta}_{1,2}\right)}{\sqrt{1+\hat{\delta}_{1,1}^{2}}\sqrt{\left(A - 2I_1\hat{\delta}_{1,1}\hat{\delta}_{1,2}\right)^2 + \left(2I_1\hat{\delta}_{1,1} + A\hat{\delta}_{1,2}\right)^2}} \quad , \tag{5.27}$$

where, $A = 1 + I_1 + \hat{\delta}_{1,1}^{2}$ and $I_k = 2I_{0k}/\left(1+I_{0k}\right)$. Parameters ξ_1 and ξ_2 describe the stagger tuning in input and output cluster and are given by:

$$\xi_1 = \left(\omega_{1,2} - \omega_{1,1}\right)/\left(\omega_s/2Q_{1,1}\right)\left(1+I_{01}\right) \quad ,$$

$$\xi_2 = \left(\omega_{2,2} - \omega_{2,1}\right) / \left(\omega_s / 2Q_{2,2}\right)\left(1 + I_{02}\right) \quad . \tag{5.28}$$

Parameter ξ describes the stagger tuning between mean frequencies of two clusters and is expressed as:

$$\xi = \left(\omega_{20} - \omega_{10}\right) / \left(\omega_s / 2Q_{2,2}\right)\left(1 + I_{02}\right) \quad . \tag{5.29}$$

Here, $\omega_{10} = \dfrac{\omega_{1,1} + \omega_{1,2}}{2}$ and $\omega_{20} = \dfrac{\omega_{2,1} + \omega_{2,2}}{2}$.

The mean frequency for four cavities is expressed as:

$$\omega_0 = \frac{\omega_{1,0} + \omega_{2,0}}{2} \quad . \tag{5.30}$$

The detuning δ is the normalized detuning between ω_s and mean frequency ω_0, and is given by:

$$\delta = \left(\omega_s - \omega_0\right) / \left(\omega_s / 2Q_{2,2}\right)\left(1 + I_{02}\right) \quad . \tag{5.31}$$

Now, in equations (5.25) - (5.27), detuning $\hat{\delta}_{k,l}$ is given by:

$$\hat{\delta}_{1,1} = \bar{Q}\left(\delta + \frac{\xi}{2}\right) + \frac{\xi_1}{2}, \qquad \hat{\delta}_{1,2} = \bar{Q}\left(\delta + \frac{\xi}{2}\right) - \frac{\xi_1}{2},$$

$$\hat{\delta}_{2,1} = \left(\delta - \frac{\xi}{2}\right) + \frac{\xi_2}{2}, \qquad \hat{\delta}_{2,1} = \left(\delta - \frac{\xi}{2}\right) + \frac{\xi_2}{2},$$

where, $\bar{Q} = \left(Q_{1,1} / Q_{2,2}\right)\left(1 + I_{02}\right)\left(1 + I_{01}\right)$. (5.32)

5.3. Results and Discussion

Based on the analytical method described above, the frequency response is studied for the two-clustered gyroklystron amplifier. A computer friendly numerical code is written to analyze the beam-wave interaction mechanism in the cluster-cavity gyroklystron.

5.3.1. Numerical Benchmarking

Table. 5.1: Design parameters for 35.12GHz, second harmonic, two-cavity gyroklystron amplifier [Zasypkin *et al.* (1996)].

Parameters	Specifications
Beam Voltage (V_b)	72kV
Beam Current (I_b)	20A
Pitch factor (α)	1.4
Magnetic Field (B_0)	0.717T
Input Cavity Length (L_1)	11.1mm
Drift Tube Length (L_{dr})	85.42mm
Output Cavity Length (L_2)	20.5mm
Quality Factor of Input Cavity (Q_1)	500
Quality Factor of Output Cavity (Q_2)	900

Table 5.1 shows the design specifications taken for the analysis of 35.12GHz second harmonic gyroklystron amplifier. The cluster-cavity concept is applied to the gyroklystron amplifier before the analysis is carried out. Firstly, each cavity of the cavity pair of clustered-cavity gyroklystron amplifier has approximately the same frequency. Secondly, Q-factors of individual cavity in the cluster are lowered to half of the conventional cavity they replace, i. e., $Q_1 = 500$, $Q_{1,1} = 250$; and $Q_2 = 900$, $Q_{2,2} = 450$. The drift space length in case of a cluster-cavity is significantly smaller than that for conventional cavity gyroklystron amplifier.

5.3.1a Analytical results

The field amplitude in the input and output cluster is calculated using equations (5.13) and (5.22). Figures 5.2(a) and 5.2(b) shows the plot of field amplitude versus frequency in case of conventional cavity and two-clustered cavity gyroklystron amplifier. It is clear from the figure that the both the input and output cluster resonate at the same

frequency, i. e., 35.05GHz which indicates the case of absence of stagger tuning between clusters. Also the bandwidth of the cluster cavity is ~0.146% which is approximately doubled than that of the conventional cavity, i. e., ~ 0.072%.

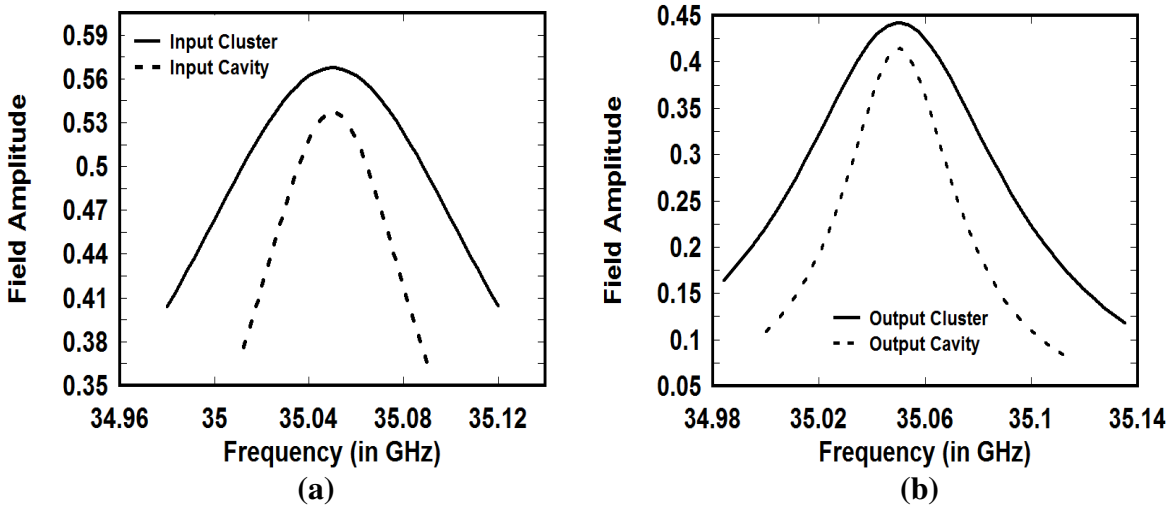

Figure. 5.2: **(a)** Field amplitude versus frequency in the input cavity and input cluster, **(b)** in the output cavity and output cluster of a conventional cavity and clustered cavity gyroklystron amplifier.

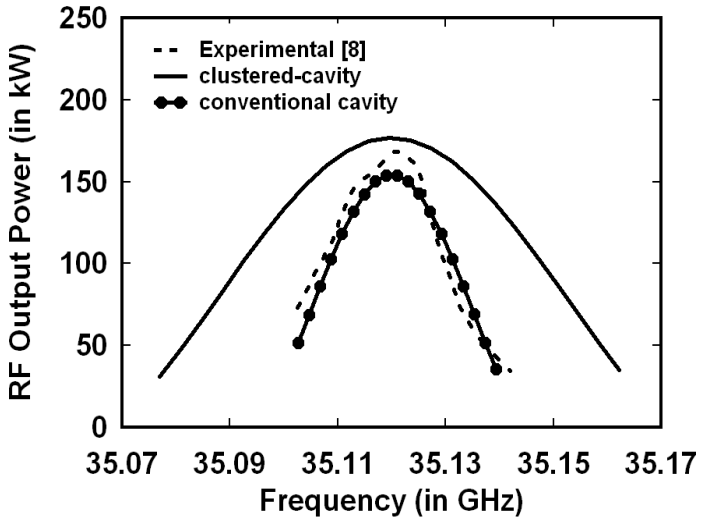

Figure. 5.3: RF output power versus frequency in case of conventional cavity [Zasypkin *et al*. (1996)] and clustered-cavity gyroklystron amplifier (for a 72kV, 14A electron beam and 3.5kW input power).

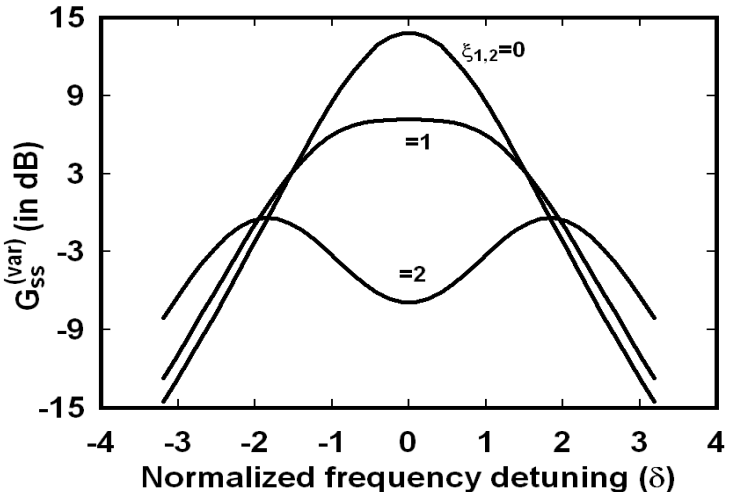

Figure. 5.4: Variable part of gain $G_{ss}^{(\mathrm{var})}$ versus normalized frequency detuning in the absence of stagger tuning between clusters (variable ξ_1 and ξ_2 indicate the stagger tuning in the input and output clusters respectively).

The bandwidth comparison in case of conventional cavity [Zasypkin *et al*. (1996)] and clustered-cavity gyroklystron amplifier is studied in Fig. 5.3. It is clear from the figure that in the cluster-cavity case, the bandwidth ~0.155% is obtained which is approximately doubled of that in the conventional cavity case, i. e., 0.08%. In the case of two-cavity clustered cavity gyroklystron amplifier, a peak RF output power of ~177kW, electronic efficiency ~17.5% and ~15.4dB gain is obtained for a 72kV, 14A electron beam and 3.5kW RF input power. Hence, by using the clustered cavity concept, the bandwidth of the device is enlarged with the slight increase in the gain of the device.

The bandwidth of the device can be further improved by stagger tuning the clustered-cavity gyroklystron amplifier. Since, there is negligible stagger tuning between clusters ($\xi \to 0$), therefore bandwidth of the device can be enhanced in terms of δ by stagger tuning between two cavities in each cluster (ξ_1 and ξ_2). Figure 5.4 shows the dependence of the variable gain $G_{ss}^{(\mathrm{var})}$ on the normalized frequency detuning δ when the stagger tuning between each cavity in a cluster is considered. The variable part of the gain

$G_{ss}^{(var)}$ is given by the equations (5.25)-(5.27). It follows from the figure that, by varying the ξ_1 and ξ_2, bandwidth gets doubled or increased by about 3.5 times though at the expense of the device gain. Thus, bandwidth of the device can be increased from 0.08% to 0.28% for the stagger tuned cluster-cavity case.

5.3.1b PIC simulation

In order to validate the analytical results described in Sec. 5.3.1a, the effect of clustered cavities on the Ka-band, two-cavity second harmonic gyroklystron amplifier [Zasypkin *et al.* (1996)], is studied using 3-D PIC simulation [CST User Manual (2013)].

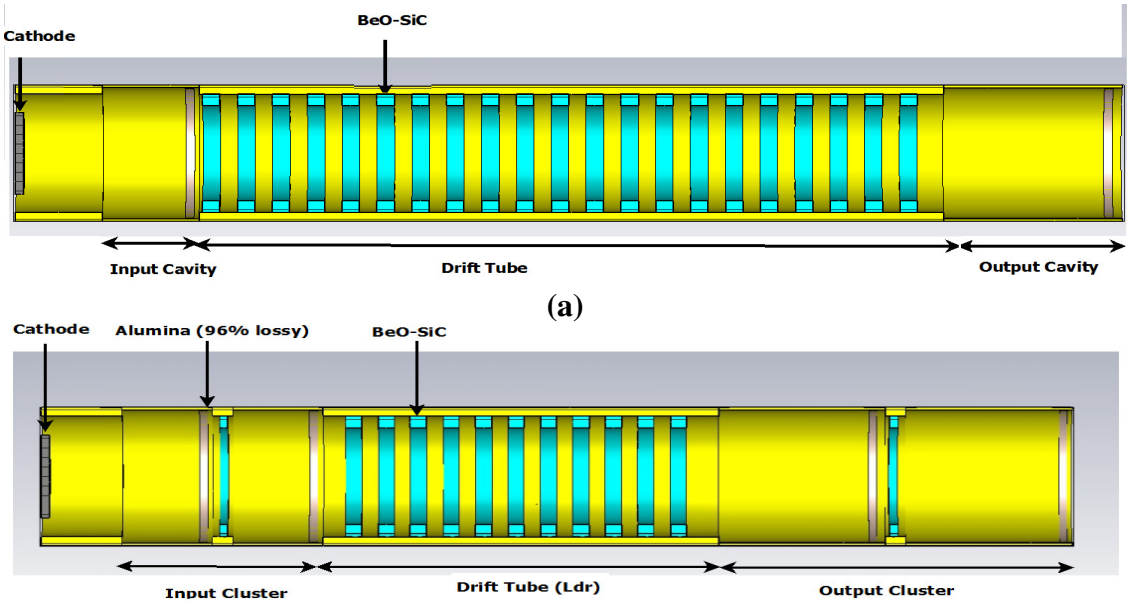

Figure. 5.5: (a) Schematic of a two-cavity conventional gyroklystron amplifier **(b)** Schematic of a two-clustered gyroklystron amplifier.

Figures. 5.5(a) and 5.5(b) shows the comparison of the 2D model of the RF interaction circuit of a two-cavity conventional, and a two-clustered gyroklystron amplifier used for the PIC simulation. The RF interaction structure has been modeled with a copper material having conductivity (σ =5.8 x 10^7 S/m). The optimum drift space length is

obtained as $L_{dr,opt}^{(2)}$ = 48.76mm; while in the conventional case L_{dr} = 85.42mm. There are important issues which need to be considered when considering clustered cavities in a gyro-amplifier. One of the major issues is the requirement to isolate the cavities in each cluster. The adjacent cavities in a cluster are loaded with lossy ceramic rings of BeO-SiC to provide the isolation between the cavities by absorbing the field leaked from cavities to the tubes. The intermediate cavities in a cluster are loaded with a lossy dielectric ring of alumina (96% loss) at a sidewall of the cavity to achieve the optimized quality factor $Q_{1,1}$ and $Q_{2,2}$. Eigenmode analysis has been performed before the PIC simulation using eigenmode solver of 'CST Microwave studio' to observe the field structure in one sub-cavity of a cluster.

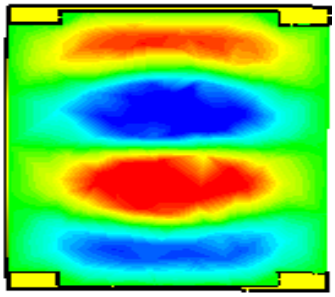

Figure. 5.6: Axial field structure of clustered-cavity subunit resonating in the TE_{02} mode.

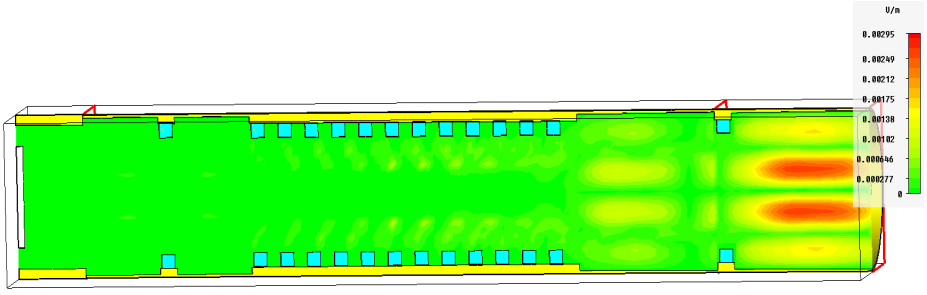

Figure. 5.7: Contour plot of the electric field pattern of TE_{02} mode along the axial length of interaction circuit.

Figure 5.6 shows axial electric field in a clustered-cavity structure subunit obtained through eigenmode study. It is clear from the figure that the cavity resonates at TE_{02} mode, which confirms the TE_{02} mode of operation of the cavity. The total loss calculation in a

cavity is accessible through 2D/3D field processing → Loss and Q calculation which includes the dielectric loss. As a result of this loss calculation, the Q factor of a cavity is available. The Q-factor in the output cavity is obtained as around 450. By following the similar procedure, the Q-factor in other cavities is calculated.

Figure 5.7 describes the contour plot of the electric field pattern of TE_{02} mode along the interaction length of the of clustered cavity gyroklystron. It is clear from the figure that, at the input cluster, minimum propagation of the RF field is observed while the RF field amplitude gradually increasing along the z-axis. The RF field strongly resonates in the output cluster forming a standing wave. Also, there is no propagation of RF field between the cavities in a cluster; hence the isolation appears to be significant.

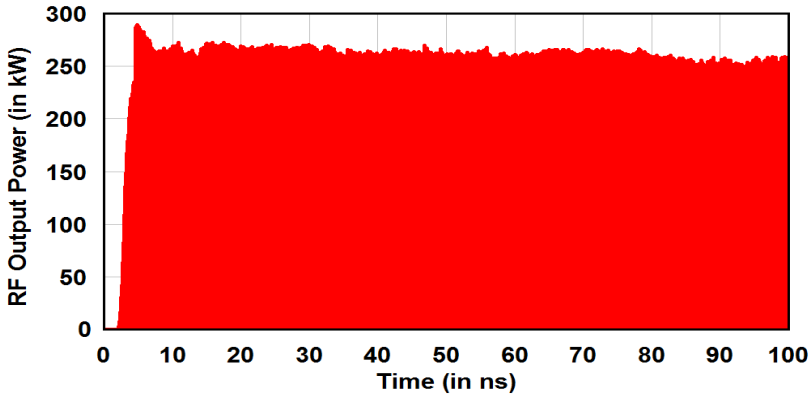

Figure. 5.8: Temporal growth of RF Output power in case of clustered cavity gyroklystron amplifier.

Figure 5.8 indicates the temporal growth of RF output power in the operating TE_{02} mode in case of clustered-cavity gyroklystron amplifier. After the temporal based processing in CST particle studio, the saturated RF output power is obtained as ~262kW in the operating mode, with ~18.2% efficiency, and ~17.02dB gain.

5.3.1c Validation

The bandwidth of the device can be determined by studying the variation of gain

with signal frequency for the design parameters shown in Table 5.1. Figure 5.9 shows the gain versus frequency in case of both conventional cavity, and clustered-cavity gyroklystron. It is clear from the figure that the bandwidth increased to ~0.155% in both clustered-cavity analysis and simulation as compared to bandwidth ~0.08% as in case of conventional cavity gyroklystron. Thus, the performance of the gyroklystron amplifier is improved in terms of gain-bandwidth product when considering the clustered-cavity device configuration.

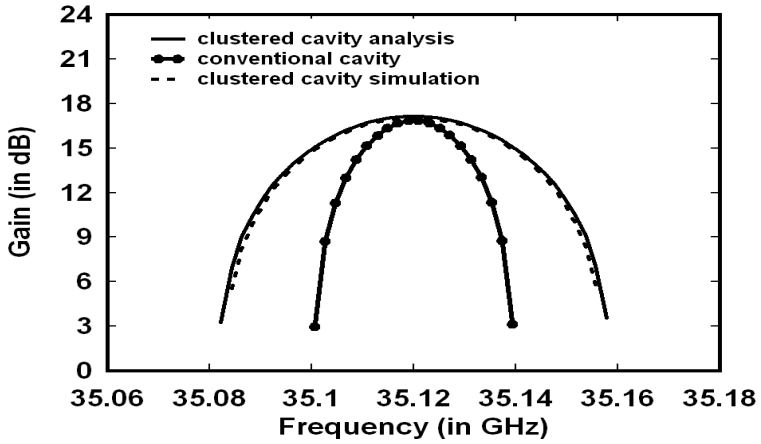

Figure. 5.9: Gain as a function of frequency in case of conventional cavity, and clustered -cavity gyroklystron.

5.4. Conclusion

The application of gyroklystron amplifier in the high-resolution advanced imaging radar should fulfill criteria of stable, high power and high bandwidth. But the existing simple cavity gyroklystron amplifier produces the higher power in a relatively narrow bandwidth and hence the performance improvement in terms of bandwidth has to be addressed. Hence in this chapter, to overcome the narrow bandwidth problem associated with the existing gyroklystron, an attempt has been made towards broadbanding of the gyroklystron by making use of a new interaction circuit, called the clustered-cavity. In this circuit, the individual intermediate cavity of a multi-cavity gyroklystron is replaced by pairs

or triplets of artificially loaded cavities which form a cluster. The *Q*-factor of each cavity in a cluster has been reduced to one-half or one-third of the single cavity resulting in either doubled or tripled bandwidth of the device. The generalized formalism for the clustered-cavity gyroklystron amplifier has been studied. Further, using this formalism a two cluster gyroklystron with two cavities in each cluster has been analyzed.

A 35.12GHz, second harmonic, two-cavity gyroklystron amplifier has been considered for its performance improvement. A peak output power of ~269kW, efficiency ~18.4% and gain ~17.14dB have been obtained in the clustered-cavity case. The bandwidth of the device has been achieved ~0.155% which is approximately doubles that of conventional cavity case, i. e., 0.08%. The results have shown that bandwidth of gyroklystron has been enhanced with the small increment in the gain, and efficiency of the device. The effect of stagger tuning on the performance of clustered-cavity gyroklystron has also been briefly studied. Further, the analytical results obtained here have been verified with the help of the PIC simulation results, and found in close agreement (within 5%) obtained from both the approaches.